AIAA JOURNAL
Vol. 41, No. 6, June 2003

Optimal Control of Laminated Shells Using Piezoelectric Sensor and Actuator Layers

M. C. Ray*
Indian Institute of Technology, Kharagpur 721 302, India

A simple method for optimal control of vibrations of simply supported thin laminated shells integrated with piezoelectric layers is presented. The piezoelectric layers act as the distributed sensors and actuators. Coupled electromechanical governing equations of motion are derived using Hamilton's variational principle. The algorithm for a linear quadratic regulator with output feedback has been employed to formulate the optimal control problem. Controlled responses for various design parameters are illustrated, and a study of the effect of variation of the central angle subtended by the shell on the performance of the actuator is presented.

Introduction

THE design of space structures, robotic manipulators, and the like requires the development of high-performing lightweight structures because of the stringent consideration of weight. The lightweight structures inherently possess low internal damping and higher flexibility and are susceptible to large vibrations with long decay time. Such structures require suitable integration of the active control means to show better performance under operation. The quest for the development of high-performing lightweight structures has led to the emerging idea of providing these structures with self-monitoring and self-controlling capabilities. Expediently, it has been found that the piezoelectric materials integrated with the flexible structures can act as distributed actuators and sensors and are able to provide these structures with self-monitoring and self-controlling capabilities. Consequently, the use of piezoelectric materials as distributed sensors and actuators has attained a great deal of importance for the purpose of active control of vibrations of beams, plates, and shells.[1–22]

It is well known that the design of an optimal controller avoids the task of arbitrarily finding the gain of the controller to meet the design objective and overcomes the problems of instability and actuator saturation.[23] The linear quadratic regulators (LQR) with either full-state feedback or output feedback are the most effective and widely used modern optimal controllers. Although the LQR with full-state feedback has some important guaranteed robustness properties in comparison with the LQR with output feedback,[24] it is difficult to measure all of the states of highly distributed systems like plates and shells. For such highly distributed systems, the implementation of the linear quadratic control with output feedback may be the most feasible means for optimal control.

A literature survey reveals that the issue of the optimal control of flexible structures using piezoelectric actuators and sensors has not been addressed in abundance and is only concerned with beam- and platelike structures.[10,12,14,15,17,18] In many practical applications, we often encounter circular cylindrical shells that are not complete in the circumferential direction. This paper focuses on the optimal control of vibrations of these types of laminated shells using distributed piezoelectric sensors and actuators. A simple method of exact solutions for linear quadratic control with output feedback is presented.

Received 2 July 2001; revision received 5 September 2002; accepted for publication 10 January 2003.

*Assistant Professor, Department of Mechanical Engineering.

Plant Model

Figure 1 demonstrates a laminated circular cylindrical shell integrated with piezoelectric layers on its top and bottom surfaces. The top piezoelectric layer acts as the distributed actuator and the bottom one as the distributed sensor. The overall structure is an N-layered laminated shell with lengthwise side a and circumferential length b. The central angle subtended by the circumferential length of the shell is θ, and the average radius of curvature of the shell is R. The shell considered here is thin and symmetric about its midplane. Hence, the classical shell theory can be employed to model the kinematics of deformations of the shell. Thus, the displacements u and v at any point in the shell along the x axis and the circumferential axis y, respectively, are given by

$$u(x, y, z) = u_0(x, y) - z\frac{\partial w}{\partial x} \tag{1a}$$

$$v(x, y, z) = \left(1 + \frac{z}{R}\right)v_0(x, y) - z\frac{\partial w}{\partial y} \tag{1b}$$

where u_0 and v_0 are the midplane displacements along the x and y axes, respectively, and w is the displacement in the radial direction z, which is constant across the thickness of the shell. The surfaces of the piezolayers that are in contact with the laminated shell substrate are suitably grounded. Thus, the electric potential function ϕ^N for the actuator layer that yields zero potential at its interface with the substrate, as well as linear variation across its thickness, is considered as[23]

$$\phi^N(x, y, z, t) = (z - h_N/h_p)\phi_0^N, \qquad h_{N+1} \geq z \geq h_N \tag{2}$$

where ϕ_0^N is the generalized electric potential coordinate and h_p is the thickness of the actuator layer.

The quasistatic constitutive equations for the piezoelectric material are[25]

$$\{D^k\} = [e]^T\{\in^k\} + [\varepsilon]\{E^k\}, \qquad k = 1 \quad \text{and} \quad N$$

$$\{\sigma^k\} = [C^k]\{\in^k\} - [e]\{E^k\}, \qquad k = 1 \quad \text{and} \quad N \tag{3}$$

and the constitutive equation for the orthotropic material of the shell substrate is given by

$$\{\sigma^k\} = [C^k]\{\in^k\}, \qquad k = 2, 3, \ldots, N-1 \tag{4}$$

where for any layer k the vectors $\{D^k\}$, $\{E^k\}$, $\{\sigma^k\}$, and $\{\in^k\}$ are the electric displacements, electric field, stress, and strain vectors, respectively. The matrices $[e]$, $[\varepsilon]$, and $[C^k]$ denote the piezoelectric, dielectric, and elastic constant matrices of the kth layer, respectively.

By the use of Eq. (1) and the application of Donnell–Mushtari shell theory, the strain displacement relations for the kth layer of the

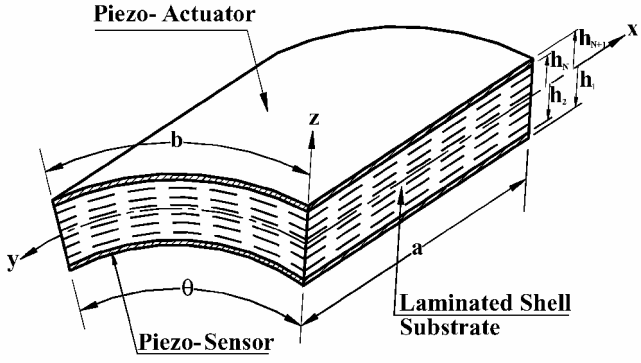

Fig. 1 Shell configuration.

shell can be written as

$$\{\in\}^k = \begin{Bmatrix} \in_{x0} \\ \in_{y0} \\ \in_{xy0} \end{Bmatrix} - z \begin{Bmatrix} k_x \\ k_y \\ k_{xy} \end{Bmatrix} \tag{5}$$

in which

$$\in_{x0} = \frac{\partial u_0}{\partial x}, \qquad \in_{y0} = \frac{\partial v_0}{\partial y} + \frac{w}{R}, \qquad \in_{xy0} = \frac{\partial u_0}{\partial y} + \frac{\partial v_0}{\partial x}$$

$$k_x = \frac{\partial^2 w}{\partial x^2}, \qquad k_y = \frac{\partial^2 w}{\partial y^2} - \frac{1}{R}\frac{\partial v_0}{\partial y}, \qquad k_{xy} = 2\frac{\partial^2 w}{\partial x \partial y} - \frac{1}{R}\frac{\partial v_0}{\partial x}$$

The electric field potential relation is given by

$$E_{x_i} = -\frac{\partial \phi^k}{\partial x_i}, \qquad x_i = x, y, z; k = 1, \qquad N \tag{6}$$

The potential energy T_p of the shell can be written as[25]

$$T_p = \frac{1}{2}\sum_{k=1}^{N}\int_{h_k}^{h_{k+1}}\int_0^b\int_0^a \{\in^k\}^T\{\sigma^k\}\mathrm{d}x\,\mathrm{d}y\,\mathrm{d}z$$

$$-\frac{1}{2}\sum_{k=1,N}\int_{h_k}^{h_{k+1}}\int_0^b\int_0^a \{E^k\}^T\{D^k\}\,\mathrm{d}x\,\mathrm{d}y\,\mathrm{d}z$$

$$-\int_0^b\int_0^a p(x, y, t)w|_{z=h_{N+1}}\,\mathrm{d}x\,\mathrm{d}y$$

$$+\int_0^b\int_0^a \bar{\sigma}(x, y, t)\phi^N|_{z=h_{N+1}}\,\mathrm{d}x\,\mathrm{d}y \tag{7}$$

and the kinetic energy T_k of the shell is

$$T_k = \frac{1}{2}\sum_{k=1}^{N}\int_{h_k}^{h_{k+1}}\int_0^b\int_0^a \rho^k(\dot{u}^2 + \dot{v}^2 + \dot{w}^2)\,\mathrm{d}x\,\mathrm{d}y\,\mathrm{d}z \tag{8}$$

where $p(x, y, t)$ is the applied load in the radial direction z, $\bar{\sigma}(x, y, t)$ is the externally applied surface charge density, ρ^k is the density of the kth layer, and each dot over a quantity represents the derivative of that quantity with respect to time t. The piezoelectric layer considered here is made of a biaxially polarized polymeric material called polyvinylidene fluoride (PVDF). The matrices $[e]$ and $[\varepsilon]$ for this piezoelectric material are given by[4]

$$[e]^T = \begin{bmatrix} 0 & 0 & 0 & 0 & 0 \\ 0 & 0 & 0 & 0 & 0 \\ e_{31} & e_{31} & 0 & 0 & 0 \end{bmatrix}, \qquad [\varepsilon] = \begin{bmatrix} \varepsilon_{11} & 0 & 0 \\ 0 & \varepsilon_{11} & 0 \\ 0 & 0 & \varepsilon_{11} \end{bmatrix} \tag{9}$$

Note here that, in the absence of an externally applied electric field, the converse piezoelectric effect in the sensor layer due to its deformation is negligible and is not considered in the evaluation of the total potential energy.

Using Eqs. (1–6) and (9) and carrying out the explicit integration with respect to z, one can express Eqs. (7) and (8) as

$$T_p = \frac{1}{2}\int_0^b\int_0^a \Big\{A_{11}\in_{x0}^2 + 2A_{12}\in_{x0}\in_{y0} + A_{22}\in_{y0}^2$$

$$+A_{66}\in_{xy0}^2 + D_{11}k_x^2 + 2D_{12}k_xk_y + D_{22}k_y^2 + D_{66}k_{xy}^2$$

$$+2e_{31}\frac{(\in_{x0} + \in_{y0}) - (h_{N+1} + h_N)(k_x + k_y)}{2}\phi_0^N$$

$$-\frac{\varepsilon_{11}}{h_p}\big(\phi_0^N\big)^2 - \frac{1}{3}h_p\varepsilon_{11}\left[\left(\frac{\partial\phi_0^N}{\partial x}\right)^2 + \left(\frac{\partial\phi_0^N}{\partial y}\right)^2\right]$$

$$-2pw + 2\bar{\sigma}\phi_0^N\Big\}\,\mathrm{d}x\,\mathrm{d}y \tag{10}$$

$$T_k = \int_0^b\int_0^a\left[m_1\big(\dot{u}_0^2 + \dot{w}^2\big) + m_2\dot{v}_0^2 + I\left(\frac{\partial\dot{w}}{\partial x}\right)^2 + I\left(\frac{\partial\dot{w}}{\partial y}\right)^2\right]\mathrm{d}x\,\mathrm{d}y \tag{11}$$

where

$$A_{ij} = \sum_{k=1}^{N}(h_{k+1} - h_k)C_{ij}^k, \qquad D_{ij} = \sum_{k=1}^{N}\frac{1}{3}\big(h_{k+1}^3 - h_k^3\big)C_{ij}^k$$

$$m_1 = \sum_{k=1}^{N}\rho^k(h_{k+1} - h_k), \qquad I = \sum_{k=1}^{N}\frac{1}{3}\rho^k\big(h_{k+1}^3 - h_k^3\big)$$

$$m_2 = m_1 + \frac{I}{R^2}$$

By application of Hamilton's variational principle,

$$\delta\int_{t_1}^{t_2}(T_k - T_p)\,\mathrm{d}t = 0 \tag{12}$$

the following coupled electromechanical governing equations of motion are obtained:

$$A_{11}\frac{\partial^2 u_0}{\partial x^2} + (A_{12} + A_{66})\frac{\partial^2 v_0}{\partial x\partial y} + A_{12}\frac{1}{R}\frac{\partial w}{\partial x}$$

$$+A_{66}\frac{\partial^2 u_0}{\partial y^2} + e_{31}\frac{\partial\phi_0^N}{\partial x} - m_1\ddot{u}_0 = 0 \tag{13}$$

$$(A_{12} + A_{66})\frac{\partial^2 u_0}{\partial x\partial y} + A_{22}\left(\frac{\partial^2 v_0}{\partial y^2} + \frac{1}{R}\frac{\partial w}{\partial y}\right) + \left(A_{66} + \frac{D_{66}}{R^2}\right)\frac{\partial^2 v_0}{\partial x^2}$$

$$-\frac{1}{R}(D_{12} + 2D_{66})\frac{\partial^3 w}{\partial x^2\partial y} - \frac{D_{22}}{R}\left(\frac{\partial^3 w}{\partial y^3} - \frac{1}{R}\frac{\partial^2 v_0}{\partial y^2}\right)$$

$$+e_{31}\left(1 + \frac{1}{2R}(h_{N+1} + h_N)\right)\frac{\partial\phi_0^N}{\partial y} - m_2\ddot{v}_0 = 0 \tag{14}$$

$$\frac{A_{12}}{R}\frac{\partial u_0}{\partial x} + \frac{A_{22}}{R}\left(\frac{\partial v_0}{\partial y} + \frac{w}{R}\right) + D_{11}\frac{\partial^4 w}{\partial x^4} + 2(D_{12} + 2D_{66})\frac{\partial^4 w}{\partial x^2\partial y^2}$$

$$+\frac{1}{R}(D_{12} + 2D_{66})\frac{\partial^3 v_0}{\partial x^2\partial y} + D_{22}\left(\frac{\partial^4 w}{\partial y^4} - \frac{1}{R}\frac{\partial^3 v_0}{\partial y^3}\right) + \frac{e_{31}}{R}\phi_0^N$$

$$-\frac{1}{2}e_{31}(h_{N+1} + h_N)\left(\frac{\partial^2\phi_0^N}{\partial x^2} + \frac{\partial^2\phi_0^N}{\partial y^2}\right)$$

$$+m_1\ddot{w} - I\left(\frac{\partial^2\ddot{w}}{\partial x^2} + \frac{\partial^2\ddot{w}}{\partial y^2}\right) = p \tag{15}$$

$$e_{31}\left(\frac{\partial u_0}{\partial x}+\frac{\partial v_0}{\partial y}+\frac{w}{R}\right)-\frac{1}{2}e_{31}(h_{N+1}+h_N)\left(\frac{\partial^2 w}{\partial x^2}+\frac{\partial^2 w}{\partial y^2}-\frac{1}{R}\frac{\partial v_0}{\partial y}\right)$$

$$-\frac{\varepsilon_{11}}{h_p}\phi_0^N+\frac{1}{3}\varepsilon_{11}h_p\left(\frac{\partial^2\phi_0^N}{\partial x^2}+\frac{\partial^2\phi_0^N}{\partial y^2}\right)+\bar{\sigma}=0 \tag{16}$$

The variational principle also yields the following simply supported boundary conditions:

1) The essential boundary conditions are

$$v_0=w=\frac{\partial w}{\partial y}=\phi_0^N=0 \tag{17a}$$

at $x=0$ and a, and

$$u_0=w=\frac{\partial w}{\partial x}=\phi_0^N=0 \tag{17b}$$

at $y=0$ and b.

2) Natural boundary conditions at the edges $x=0$ and a are

$$A_{11}\frac{\partial u_0}{\partial x}+A_{12}\left(\frac{\partial v_0}{\partial y}+\frac{w}{R}\right)+e_{31}\phi_0^N=0$$

$$D_{11}\frac{\partial^2 w}{\partial x^2}+D_{12}\left(\frac{\partial^2 w}{\partial y^2}-\frac{1}{R}\frac{\partial v_0}{\partial y}\right)-\frac{1}{2}e_{31}(h_{N+1}+h_N)\phi_0^N=0 \tag{18}$$

3) Natural boundary conditions at the edges $y=0$ and b are

$$A_{12}\frac{\partial u_0}{\partial x}+A_{22}\left(\frac{\partial v_0}{\partial y}+\frac{w}{R}\right)-\frac{D_{12}}{R}\frac{\partial^2 w}{\partial x^2}$$

$$-\frac{D_{22}}{R}\left(\frac{\partial^2 w}{\partial y^2}-\frac{1}{R}\frac{\partial v_0}{\partial y}\right)+e_{31}\phi_0^N=0$$

$$D_{12}\frac{\partial^2 w}{\partial x^2}+D_{22}\left(\frac{\partial^2 w}{\partial y^2}-\frac{1}{R}\frac{\partial v_0}{\partial y}\right)-\frac{1}{2}e_{31}(h_{N+1}+h_N)\phi_0^N=0 \tag{19}$$

The surfaces of the piezoelectric layers are fully electroplated and can be treated as capacitors with the piezoelectric layer as the dielectric medium between these parallel surface electrodes. Thus, the uniform voltage V across these parallel electrodes due to the applied surface charge density $\bar{\sigma}$ on one of the electrodes, with the other electrode being grounded, can be given by[18]

$$V=\bar{\sigma}ab/C_p \tag{20}$$

where C_p is the capacitance of the piezoelectric actuator layer.

Following Navier's method, the unknown displacement variables u_0, v_0, w, and the generalized electric potential coordinate ϕ_0^N are expressed in the following double Fourier series representations:

$$u_0(x,y,t)=\sum_{m=1}^{\infty}\sum_{n=1}^{\infty}U_{mn}(t)\cos\alpha x\sin\beta y$$

$$v_0(x,y,t)=\sum_{m=1}^{\infty}\sum_{n=1}^{\infty}V_{mn}(t)\sin\alpha x\cos\beta y$$

$$w(x,y,t)=\sum_{m=1}^{\infty}\sum_{n=1}^{\infty}W_{mn}(t)\sin\alpha x\sin\beta y$$

$$\phi_0^N(x,y,t)=\sum_{m=1}^{\infty}\sum_{n=1}^{\infty}\Phi_{mn}(t)\sin\alpha x\sin\beta y \tag{21}$$

in which $\alpha=m\pi/a$ and $\beta=n\pi/b$; $U_{mn}(t)$, $V_{mn}(t)$, and $W_{mn}(t)$; and $\Phi_{mn}(t)$ are the unknown temporal functions to be determined such that the governing equations are satisfied at any point in the continuum. It is evident that these expressions satisfy the boundary conditions given by Eqs. (17–19). Accordingly, the load function and the applied uniform voltage are also expressed in the same manner as

$$p(x,y,t)=\sum_{m=1}^{\infty}\sum_{n=1}^{\infty}Q_{mn}(t)\sin\alpha x\sin\beta y$$

$$V(x,y,t)=\sum_{m=1}^{\infty}\sum_{n=1}^{\infty}\bar{V}_{mn}(t)\sin\alpha x\sin\beta y \tag{22}$$

where $Q_{mn}(t)$ and $\bar{V}_{mn}(t)$ are the time-dependent modal amplitudes of the applied load and control voltage, respectively. Substituting Eqs. (20–22) into Eqs. (13–16), one obtains

$$\bar{m}\ddot{U}_{mn}(t)+S_{11}U_{mn}(t)+S_{12}V_{mn}(t)+S_{13}W_{mn}(t)+S_{14}\Phi_{mn}(t)=0 \tag{23}$$

$$\bar{m}\ddot{V}_{mn}(t)+S_{21}U_{mn}(t)+S_{22}V_{mn}(t)+S_{23}W_{mn}(t)+S_{24}\Phi_{mn}(t)=0 \tag{24}$$

$$M\ddot{W}_{mn}(t)+S_{31}U_{mn}(t)+S_{32}V_{mn}(t)+S_{33}W_{mn}(t)+S_{34}\Phi_{mn}(t)=Q_{mn}(t) \tag{25}$$

$$S_{41}U_{mn}(t)+S_{42}V_{mn}(t)+S_{43}W_{mn}(t)+S_{44}\Phi_{mn}(t)+(C_p/ab)ab=0 \tag{26}$$

The various coefficients S_{ij}, $i,j=1,2,3,4$, and M appearing in Eqs. (23–26) are shown in the Appendix. When the inertias[26] are neglected due to in-plane motions $\dot{u}_0$ and $\dot{v}_0$ the following single governing equation of motion describing the open-loop dynamics of the shell can be derived from Eqs. (23–26):

$$\ddot{W}_{mn}(t)+\omega_{mn}^2W_{mn}(t)=[Q_{mn}(t)/M]-K_c\bar{V}_{mn}(t) \tag{27}$$

in which the expressions for ω_{mn}^2 and K_c are presented in the Appendix.

Sensor Output

When the sensor layer deforms along with the substrate, electric charge is induced in it because of the direct piezoelectric effect. This induced charge can be collected on the ungrounded exposed electroplated surface of the sensor. According to the Gauss law, this charge $q(t)$ is equal to the spatial integration of the electric displacement in the z direction over that electroplated surface, and it can be evaluated as follows[27]:

$$q(t)=\int_0^b\int_0^a D_z\Big|_{z=h_1}\,\mathrm{d}x\,\mathrm{d}y \tag{28}$$

Using Eqs. (1), (3), and (21) in Eq. (28), one can express the output charge from the sensor as

$$q(t)=\sum_{m=1}^{\infty}\sum_{n=1}^{\infty}q_{mn}(t)=\sum_{m=1}^{\infty}\sum_{n=1}^{\infty}F_{mn}W_{mn}(t) \tag{29}$$

where

$$F_{mn}=(e_{31}/\alpha\beta)[h_1(\alpha^2+\beta^2)-\alpha-(1+h_1/R)\beta+1/R][1-(-1)^m][1-(-1)^n]$$

The resulting modal current induced by the sensor can be determined as

$$i_{mn}(t)=\frac{\mathrm{d}q_{mn}(t)}{\mathrm{d}t}=F_{mn}\dot{W}_{mn}(t) \tag{30}$$

Optimal Control with Output Feedback

To formulate the optimal control problem, the applied mechanical load is considered to be absent and Eq. (27) is represented in the standard state-space form as

$$\frac{\mathrm{d}X(t)}{\mathrm{d}t} = AX(t) + B\bar{V}_{mn}(t) \tag{31}$$

where

$$X(t) = [W_{mn}(t) \quad \dot{W}_{mn}(t)/\omega_{mn}]^T, \qquad A = \begin{bmatrix} 0 & \omega_{mn} \\ -\omega_{mn} & 0 \end{bmatrix}$$

$$B = [0 \quad -K_c/\omega_{mn}]^T$$

In the closed-loop model, the current output from the sensor as given by Eq. (30) is negatively fed back to the actuator. This results in the generation of a surface charge on the electrode-covered surface of the actuator, which, after uniform distribution, gives rise to a uniform control voltage across the electrodes of the actuator layer. Thus, in the closed-loop system, the modal control voltage input to the actuator can be expressed as

$$V_{mn}(t) = -Ki_{mn}(t) = -KC_0X \tag{32}$$

where K is the optimal gain to be determined and $C_0 = [0 \quad F_{mn}\omega_{mn}]$.

Note from Eq. (32) that the feedback of the output from the sensor generates the control law with reduced state information as manifested by the output matrix C_0. Hence, the optimal control problem turns out to be an LQR problem with output feedback. The optimal regulation of the state may be attained by selecting the control input $\bar{V}_{mn}(t)$ to minimize a performance index[23]:

$$J = \int_0^\infty \{X(t)^T QX(t) + \bar{V}_{mn}(t)^T r\bar{V}_{mn}(t)\}\,\mathrm{d}t \tag{33}$$

where J is the cost function and Q and r the positive semidefinite state weighting matrix and positive-definite control weighting matrix, respectively. If the closed-loop plant is asymptotically stable, then it is well known that the minimization of the performance index given by Eq. (33) leads to minimizing the cost function of the form

$$J = \tfrac{1}{2}tr\{PX(0)X(0)^T\}, \qquad P \geq 0 \tag{34}$$

in which P is an unknown symmetric positive-semidefinite matrix. To relieve Eq. (34) of its dependence on the initial state $X(0)$, the problem statement is usually modified to that of minimizing the expected value of J, that is, $E(J)$. Equation (34) should then be replaced by

$$E(J) = \tfrac{1}{2}\mathrm{tr}(PY) \tag{35}$$

where Y is the autocorrelation of initial state vector. In general, the initial states are assumed to be uniformly distributed on the unit sphere, such that Y is an identity matrix.[28]

The procedure of minimization yields the following design equations[23]:

$$A_c^T P + PA_c + C_0^T K^T RKC_0 + Q = 0 \tag{36}$$

$$SA_c^T + A_cS + Y = 0 \tag{37}$$

$$K = R^{-1}B^T PSC_0^T\left(C_0SC_0^T\right)^{-1} \tag{38}$$

wherein $A_c = A - BKC_0$. The unknown matrices P and S are solved from Eqs. (36) and (37), and the optimal value of K is obtained from Eq. (38). The following algorithm[29] is employed to obtain the iterative solutions of Eqs. (36) and (37):

1) Choose the initial value of K as $-\omega_{mn}/(K_cF_{mn})$, such that A_c is asymptotically stable. Set $i = 0$.

2) Solve Eqs. (36) and (37) for P_i and S_i.

3) Evaluate $\Delta K_i = R^{-1}B^T PSC_0^T(C_0SC_0^T)^{-1} - K_i$.

4) Set $K_{i+1} = K_i + \lambda\Delta K_i$, where λ is chosen at each iteration such that $J_{i+1} < J_i$.

5) Set $i = i + 1$, go to step 2, and repeat the process until convergence is achieved.

Results

By the use of Eq. (32), Eq. (27) is solved. Finally, by the use of Eq. (21), the exact solution for the radial displacement w at any point of the shell can be obtained as

$$w(x, y, t) = \sum_{m=1}^{\infty}\sum_{n=1}^{\infty} e^{\alpha_{mn}t}\frac{\cos\beta_{mn}t - \alpha_{mn}\sin\beta_{mn}t}{\beta_{mn}} \times W_{mn}(0)\sin\alpha x\sin\beta y \tag{39}$$

where, for each combination of m and n, the real and imaginary parts α_{mn} and β_{mn}, respectively, of the optimal closed-loop poles are given by

$$\alpha_{mn} = \tfrac{1}{2}KK_cF_{mn}, \qquad \beta_{mn} = \tfrac{1}{2}\sqrt{4\omega_{mn}^2 - K^2K_c^2F_{mn}^2}$$

and $W_{mn}(0)$ is the initial deflection at the center of the shell. Numerical results are sought for a (0/90/0 deg) laminated shell for which $a = 0.5$ m, $\theta = 30$ deg, and $b = a$. Each ply of the laminate is made of a graphite/epoxy composite, for which the following material properties are used:

$$E_L = 172.5\ \text{GPa}, \qquad E_T = E_L/25, \qquad G_{LT} = 0.5E_T$$

$$G_{TT} = 0.2E_T, \qquad \upsilon_{LT} = \upsilon_{TT} = 0.25, \qquad \rho = 1600\ \text{kg/m}^2$$

where E_L and E_T are Young's moduli, G_{LT} and G_{TT} are the shear moduli, and υ_{LT} and υ_{TT} are major and minor Poisson's ratios. L and T designate the longitudinal and transverse principal material directions, respectively. The material properties of PVDF[4,18] are adopted as

$$E = 2 \times 10^9\ \text{Pa}, \qquad e_{31} = 0.046\ \text{C/m}^2$$

$$\varepsilon_{11} = \varepsilon_{22} = \varepsilon_{33} = 1.062 \times 10^{-10}\ \text{F/m}$$

$$C_p = 3.8 \times 10^{-6}\ \text{F}, \qquad \rho = 1800\ \text{kg/m}^2$$

The thickness of each ply of the substrate is taken as 1 mm, and that of each piezoelectric layer is 0.5 mm. The state weighting matrix Q is considered as $q\omega_{mn}^2C_0^TC_0/(K_c^2F_{mn}^2)$, with q being the design parameter. The typical curve in Fig. 2 demonstrates that the cost function converges to a minimum value after a certain number of iterations, yielding the optimal gain for $m = 1$ and $n = 1$. A uniformly distributed load of 1000 N/m^2 is applied statically on the top of the shell and then withdrawn to set the shell into transient vibration

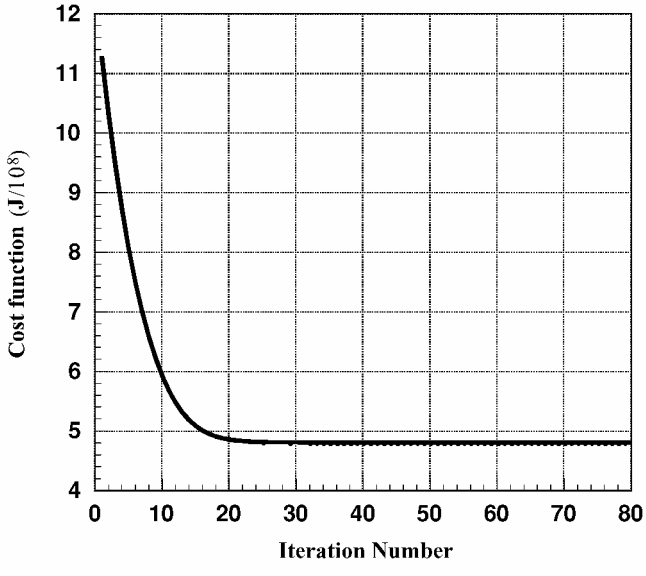

Fig. 2 Convergence of cost function for $m = 1$ and $n = 1$ ($q = 0.01$, $r = 0.2$, $\theta = 30$ deg, and $b = a$).

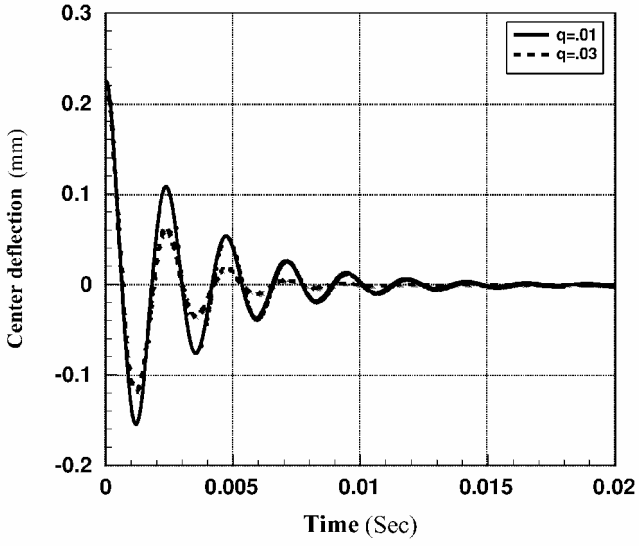

Fig. 3 Center deflection for different values of q ($r = 0.2$, $\theta = 30$ deg, and $b = a$).

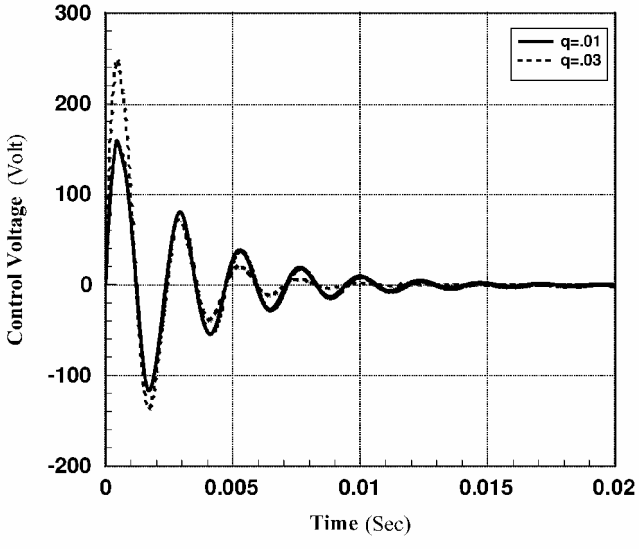

Fig. 4 Control voltage for different values of q ($r = 0.2$, $\theta = 30$ deg, and $b = a$).

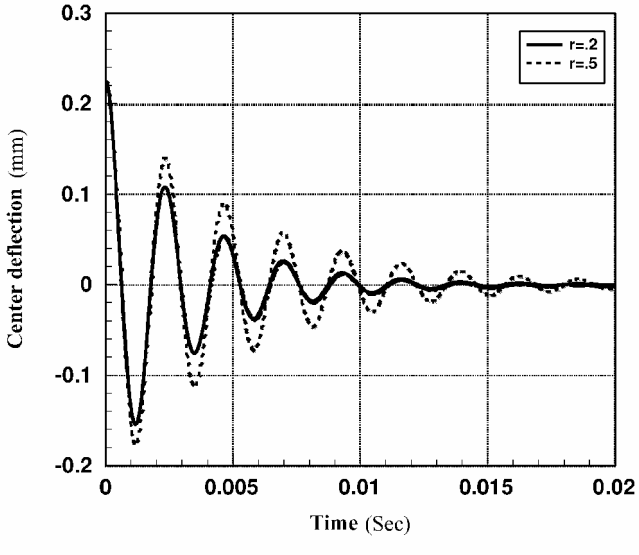

Fig. 5 Center deflection for different values of r ($q = 0.01$, $\theta = 30$ deg, and $b = a$).

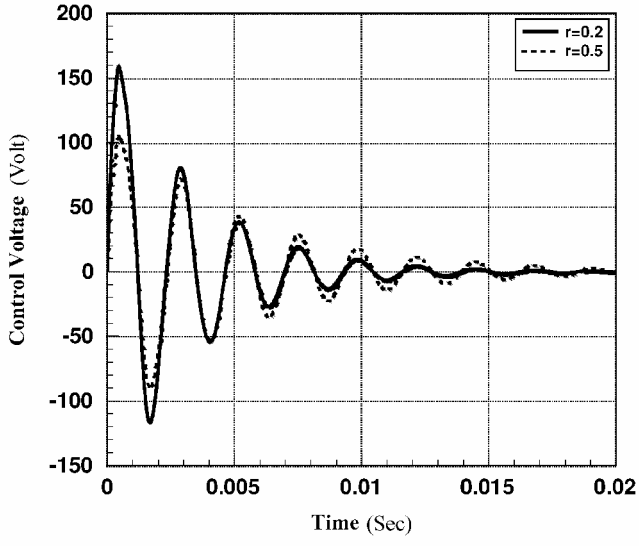

Fig. 6 Control voltage for different values of r ($q = 0.01$, $\theta = 30$ deg, and $b = a$).

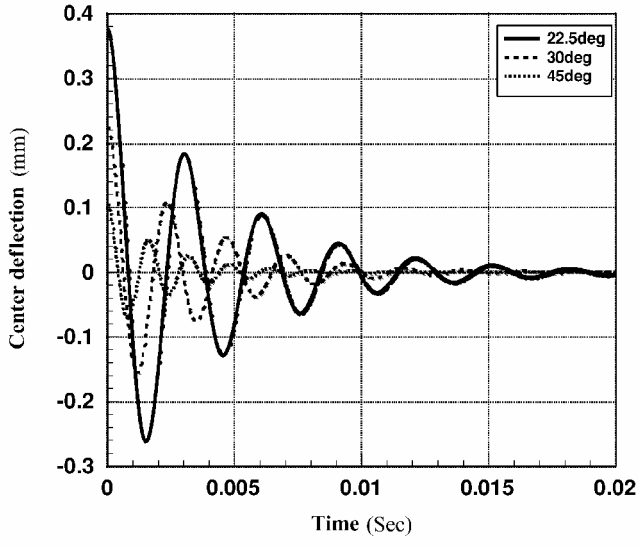

Fig. 7 Center deflection for different values of central angle θ ($q = 0.01$, $r = 0.2$, and $b = a$).

with initial deflections. To test the convergence of the solution, the contribution of the higher modes into the controlled response is investigated. It has been noted that the solutions are rapidly convergent and only the first few terms ($m = 7$ and $n = 7$) of the series [Eq. (21)] are needed for convergence. Figure 3 illustrates the control of center deflection. The role of design parameters q and r is obvious. For a fixed value of r as the value of q, that is, as the weighting on the state increases, the initial control voltage increases (Fig. 4), and the settling time decreases. Note from Fig. 3 that the damping factor increases from 0.11 to 0.21 due to the variation of the design parameters. On the other hand, for a particular value of q, as the value of r increases, the regulator takes longer time to drive the state to zero as shown in Fig. 5. In this case, the control voltage is initially less than that for the lower value of r as shown in Fig. 6 and the value of damping factor decreases from 0.11 to 0.071 (Fig. 5). Figures 7 and 8 illustrate the effect of variation of the central angle, θ subtended by the shell, whereas the values of a and b remain constant. It can be observed from Figs. 7 and 8 that as the value of θ decreases, that is, the radius of curvature increases, the actuator needs higher control voltage (Fig. 8). This is because when the radius of curvature increases, the shell becomes more flexible,[30] as shown in Fig. 7.

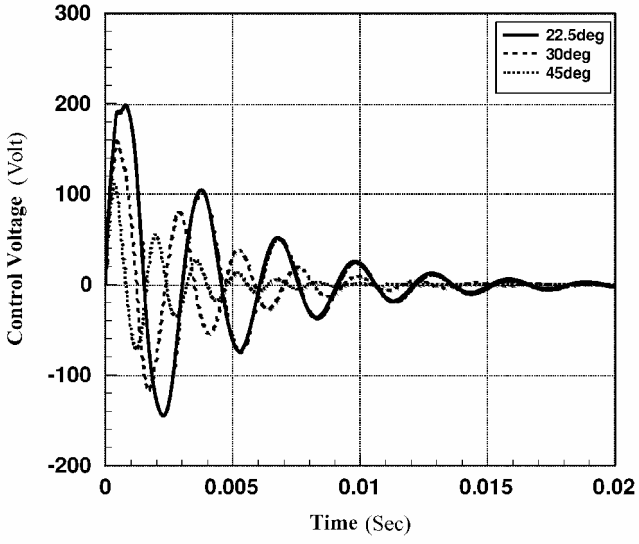

Fig. 8 Control voltage for different values of central angle θ ($q = 0.01$, $r = 0.2$, and $b = a$).

Conclusions

This paper focuses on the derivation of a simple method for optimal control of vibrations of thin, simply supported, laminated circular cylindrical shells integrated with piezoelectric layers. The piezoelectric layers act as the distributed sensors and actuators. The shells considered here are not full in the circumferential direction. Coupled electromechanical governing equations of motions are derived using Hamilton's variational principle. Emphasis is placed on obtaining the exact solutions of these governing equations while formulating an optimal control problem. The optimal controller is an LQR with output feedback. Controlled responses are obtained for a shell with stacking sequence (0/90/0 deg), and the role of various design parameters has been studied. Also, an attempt has been made to demonstrate the effect of variation of the central angle subtended by the shell for a particular case of $b = a$. The actuator needs higher control voltage as the value of the angle decreases. The proposed method may be extended to the optimal control of laminated cylindrical shells with other stacking sequences. The results may be useful for the purpose of validating the other numerical models for which the exact solutions are not possible.

Appendix: Coefficients and Parameters

The coefficients S_{ij}, $i, j = 1, 2, 3, 4$, and M appearing in Eqs. (23–26) and the parameters ω_{mn}^2 and K_c appearing in Eq. (27) are given by

$$S_{11} = A_{11}\alpha^2 + A_{66}\beta^2, \qquad S_{12} = (A_{12} + A_{66})\alpha\beta$$

$$S_{13} = -\frac{A_{12}\alpha}{R}, \qquad S_{14} = -e_{31}\alpha, \qquad S_{21} = S_{12}$$

$$S_{22} = \left(\frac{A_{66} + D_{66}}{R^2}\right)\alpha^2 + \left(\frac{A_{22} + D_{22}}{R^2}\right)\beta^2$$

$$S_{23} = -\frac{\{A_{22}\beta + (D_{12} + 2D_{66})\alpha^2\beta + D_{22}\beta^3\}}{R}$$

$$S_{24} = -e_{31}\left\{1 + \frac{h_{N+1} + h_N}{(2R)}\right\}\beta$$

$$S_{31} = S_{13}, \qquad S_{32} = S_{23}$$

$$S_{33} = D_{11}\alpha^4 + 2(D_{12} + 2D_{66})\alpha^2\beta^2 + D_{22}\beta^4 + \frac{A_{22}}{R^2}$$

$$S_{34} = e_{31}\left\{\frac{1}{R} + \frac{(h_{N+1} + h_N)(\alpha^2 + \beta^2)}{2}\right\}$$

$$S_{41} = S_{14}, \qquad S_{42} = S_{24}, \qquad S_{43} = S_{34}$$

$$S_{44} = -\varepsilon_{11}\left\{\frac{h_p(\alpha^2 + \beta^2)}{3} + \frac{1}{h_p}\right\}, \qquad M = \bar{m} + I(\alpha^2 + \beta^2)$$

$$\omega_{mn}^2 = \frac{E_{33} - c_1 E_{31} - c_3 E_{32}}{M}, \qquad E_{31} = \frac{S_{31} - S_{34}S_{41}}{S_{44}}$$

$$E_{32} = \frac{S_{32} - S_{34}S_{42}}{S_{44}}, \qquad E_{33} = \frac{S_{33} - S_{34}S_{43}}{S_{44}}$$

$$K_c = -\frac{S_{34}C_p/ab + c_2 E_{31} + c_4 E_{32}}{M}, \qquad c_1 = \frac{E_{13}E_{22} - E_{23}E_{12}}{E_{11}E_{22} - E_{21}E_{12}}$$

$$c_2 = \frac{C_p(E_{12}S_{24} - E_{22}S_{14})}{S_{44}ab(E_{11}E_{22} - E_{21}E_{12})}, \qquad c_3 = \frac{E_{13}E_{21} - E_{23}E_{11}}{E_{12}E_{21} - E_{11}E_{22}}$$

$$c_4 = \frac{C_p(E_{11}S_{24} - E_{21}S_{14})}{S_{44}ab(E_{12}E_{21} - E_{11}E_{22})}, \qquad E_{11} = \frac{S_{11} - S_{14}S_{41}}{S_{44}}$$

$$E_{12} = \frac{S_{12} - S_{14}S_{42}}{S_{44}}, \qquad E_{13} = \frac{S_{13} - S_{14}S_{43}}{S_{44}}$$

$$E_{21} = \frac{S_{21} - S_{24}S_{41}}{S_{44}}, \qquad E_{22} = \frac{S_{22} - S_{24}S_{42}}{S_{44}}$$

$$E_{23} = \frac{S_{23} - S_{24}S_{43}}{S_{44}}$$

References

[1]Bailey, T., and Hubbard, J. E., "Distributed Piezoelectric Polymer Active Vibration Control of a Cantilever Beam," *Journal of Guidance, Control, and Dynamics*, Vol. 8, No. 5, 1985, pp. 605–611.

[2]Crawley, E. F., and Luis, J. D., "Use of Piezoelectric Actuators as Elements of Intelligent Structures," *AIAA Journal*, Vol. 25, No. 10, 1987, pp. 1373–1385.

[3]Baz, A., and Poh, S., "Performance of an Active Control System with Piezoelectric Actuators," *Journal of Sound and Vibration*, Vol. 126, No. 2, 1988, pp. 327–343.

[4]Tzou, H. S., and Tseng, C. I., "Distributed Piezoelectric Sensor/Actuator Design for Dynamic Measurement/Control of Distributed Parameter Systems: A Piezoelectric Finite Element Approach," *Journal of Sound and Vibration*, Vol. 138, No. 1, 1990, pp. 17–34.

[5]Lee, C. K., and Moon, F. C., "Laminated Piezopolymer Plates for Torsion and Bending Sensors and Actuators," *Journal of the Acoustical Society of America*, Vol. 85, No. 6, 1989, pp. 2432–2439.

[6]Lee, C. K., Chiang, W. W., and Sullivan, O., "Piezoelectric Modal Sensor/Actuator Pairs for Critical Active Damping Vibration Control," *Journal of the Acoustical Society of America*, Vol. 90, No. 1, 1991, pp. 374–383.

[7]Hanagud, S., Obal, M. W., and Calise, A. J., "Optimal Vibration Control by the Use of Piezoceramic Sensors and Actuators," *Journal of Guidance, Control, and Dynamics*, Vol. 15, No. 5, 1992, pp. 1199–1206.

[8]Chandrashekara, K., and Agarwal, A. N., "Active Vibration Control of Laminated Composite Plates Using Piezoelectric Devices: A Finite Element Approach," *Journal of Intelligent Material Systems and Structures*, Vol. 4, No. 4, 1993, pp. 496–508.

[9]Samanta, B., Ray, M. C., and Bhattacharyya, R., "Finite Element Model for Active Control of Intelligent Structures," *AIAA Journal*, Vol. 34, No. 9, 1996, pp. 1885–1893.

[10]Baz, A., and Poh, S., "Optimal Vibration Control with Modal Positive Position Feedback," *Optimal Control Applications and Methods*, Vol. 17, 1996, pp. 141–149.

[11]Kang, Y. K., Park, H. C., Hwang, W. W., and Han, K. S., "Optimum Placement of Piezoelectric Sensor/Actuator for Vibration Control of Laminated Beams," *AIAA Journal*, Vol. 34, No. 9, 1996, pp. 1921–1926.

[12]Yang, S. M., and Lee, Y. J., "Optimization of Non-Collocated Sensor/Actuator Location and Feedback Gain in Control Systems," *Smart Materials and Structures*, Vol. 2, No. 2, 1993, pp. 96–102.

[13]Chandrashekhara, K., and Varadarajan, S., "Adaptive Shape Control of Composite Beams with Piezoelectric Actuators," *Journal of Intelligent Material Systems and Structures*, Vol. 8, No. 2, 1997, pp. 112–119.

[14]Kim, Y., Kum, D., and Nam, C., "Simultaneous Structural/Control Optimum Design of Composite Plate with Piezoelectric Actuators," *Journal of Guidance, Control, and Dynamics*, Vol. 20, No. 6, 1997, pp. 1111–1116.

[15]Chen, C. Q., and Shen, Y., "Optimal Control of Active Structures with Piezoelectric Sensor and Actuators," *Smart Materials and Structures*, Vol. 6, No. 4, 1997, pp. 403–411.

[16]Han, J. H., and Lee, I., "Analysis of Composite Plates with Piezoelectric Actuators for Vibration Control Using Layerwise Displacement Theory," *Composites, Part B, Engineering*, Vol. 29, No. 5, 1998, pp. 621–630.

[17]Tong, D., Williams, I. I., Robert, L., and Agarwal, S. K., "Optimal Shape Control of Composite Thin Plates with Piezoelectric Actuators," *Journal of Intelligent Material Systems and Structures*, Vol. 9, No. 6, 1998, pp. 458–454.

[18]Ray, M. C., "Optimal Control of Laminated Plates with Piezoelectric Sensor and Actuator Layers," *AIAA Journal*, Vol. 36, No. 12, 1998, pp. 2204–2208.

[19]De Almedia, S. M., "Shape Control of Laminated Plates Piezoelectric Actuators Including Stress-Stiffening Effects," *AIAA Journal*, Vol. 37, No. 8, 1999, pp. 1017–1023.

[20]Zhou, Y. H., Wang, J., Zheng, X. J., and Jiang, Q., "Vibration Control of Variable Thickness Plates with Piezoelectric Sensors and Actuators Based on Wavelet Theory," *Journal of Sound and Vibration*, Vol. 237, No. 3, 2000, pp. 395–410.

[21]Balamurugan, V., and Narayanan, S., "Active Vibration Control of Smart Shell Using Distributed Piezoelectric Sensors and Actuators," *Smart Materials and Structures*, Vol. 10, No. 2, 2001, pp. 173–180.

[22]Newbury, K. M., and Leo, D. J., "Structural Dynamics of Stiffened Plates with Piezoceramic Sensors and Actuators," *AIAA Journal*, Vol. 39, No. 5, 2001, pp. 942–950.

[23]Ray, M. C., Bhattacharyya, R., and Samanta, B., "Exact Solutions for Static Analysis of Intelligent Structures," *AIAA Journal*, Vol. 31, No. 9, 1993, pp. 1684–1691.

[24]Lewis, F. L., *Applied Optimal Control and Estimation*, Prentice–Hall, Englewood Cliffs, NJ, 1992, Chap. 4.

[25]Tiersten, H. F., *Linear Piezoelectric Plate Vibrations*, Plenum, New York, 1969, Chap. 6.

[26]Leissa, A. W., and Kadi, A. S., "Curvature Effects on Shallow Shells," *Journal of Sound and Vibration*, Vol. 16, No. 2, 1971, pp. 173–187.

[27]Griffiths, D. J., *Introduction to Electrodynamics*, Prentice–Hall of India, New Delhi, India, 1991, Chap. 4.

[28]Levine, W. S., and Athans, M., "On the Determination of the Optimal Constant Output Feedback Gains for Linear Multivariable Systems," *IEEE Transactions on Automatic Control*, Vol. AC-15, 1970, pp. 44–48.

[29]Moerder, D. D., and Calise, A. J., "Convergence of a Numerical Algorithm for Calculating Optimal Output Feedback Gains," *IEEE Transactions on Automatic Control*, Vol. AC-30, 1985, pp. 900–903.

[30]Timoshenko, S. P., and Woinowsky-Kreiger, S., *Theory of Plates and Shells*, McGraw–Hill, New York, 1959, Chap. 15.

A. M. Baz
Associate Editor